Relationship Between Scleral Thickness and Choroidal Structure in Central Serous Chorioretinopathy

Naoya Imanaga,[1] Nobuhiro Terao,[1] Shozo Sonoda,[2] Shota Sawaguchi,[1] Yukihide Yamauchi,[1] Taiji Sakamoto,[2] and Hideki Koizumi[1]

[1]Department of Ophthalmology, Graduate School of Medicine, University of the Ryukyus, Okinawa, Japan
[2]Department of Ophthalmology, Kagoshima University Graduate School of Medical and Dental Sciences, Kagoshima, Japan

Correspondence: Hideki Koizumi, Department of Ophthalmology, Graduate School of Medicine, University of the Ryukyus, 207 Uehara, Nishihara-cho, Nakagami-gun, 903-0215 Okinawa, Japan;
hkoizumi@med.u-ryukyu.ac.jp

Received: May 15, 2022
Accepted: December 30, 2022
Published: January 20, 2023

Citation: Imanaga N, Terao N, Sonoda S, et al. Relationship between scleral thickness and choroidal structure in central serous chorioretinopathy. *Invest Ophthalmol Vis Sci.* 2023;64(1):16. https://doi.org/10.1167/iovs.64.1.16

Purpose. Central serous chorioretinopathy (CSC) is a retinal disorder characterized by serous retinal detachment with or without pigment epithelial detachment in the posterior pole of the eye. We aimed to elucidate the relationship between scleral thickness and choroidal structure in CSC eyes.

Methods. This single-center retrospective study included 111 eyes of 111 CSC patients. Using swept-source optical coherence tomography, the horizontal cross-sectional images of the posterior choroid were converted to binary images by semiautomated software. The luminal and stromal areas of the choroid were measured, and the luminal/stromal (L/S) ratios of the whole choroid (WC), inner choroid, and outer choroid (OC) at 1500 µm, 3000 µm, and 7500 µm ranges centered on the fovea were calculated. Correlations of L/S ratio and age, spherical equivalent, axial length, subfoveal choroidal thickness (SCT), and scleral thickness were determined. Scleral thickness was measured vertically, 6 mm posterior to the scleral spur in four directions.

Results. SCT and mean scleral thickness were significantly positively correlated with the L/S ratio in all ranges of WC and OC. Multiple regression analysis found that SCT and mean scleral thickness were significantly correlated with the L/S ratio, and the strength of correlation of mean scleral thickness (WC: 0.386, $P < 0.001$; OC: 0.391, $P < 0.001$) was greater than that of SCT (WC: 0.368, $P < 0.001$; OC: 0.383, $P < 0.001$) in 7500 µm range.

Conclusions. Thick sclera appeared to play a role in an increase in the luminal component of the posterior choroid in CSC eyes.

Keywords: anterior-segment optical coherence tomography, central serous chorioretinopathy, choroidal structure, choroidal thickness, pachychoroid, scleral thickness, swept-source optical coherence tomography

Central serous chorioretinopathy (CSC), a pachychoroid spectrum disease, is a retinal disorder characterized by serous retinal detachment (SRD) with or without pigment epithelial detachment in the posterior pole of the eye.[1,2] CSC commonly occurs in middle-aged men.[3–5] Furthermore, type-A personality,[6] psychological stress,[7] steroid use,[8] pregnancy,[9] hyperopic refractive error,[5,10,11] short axial length (AL),[10,11] and certain genetic factors[12–16] are widely regarded as risk factors for CSC. Since Gass[17] proposed choroidal abnormality as the primary cause of pathogenesis in CSC, many clinical imaging studies focusing on the choroid have been conducted. In particular, several studies using indocyanine green angiography (ICGA) have found delayed filling of the choriocapillaris, dilated choroidal vessels, and choroidal vascular hyperpermeability in CSC.[18–22] These ICGA findings suggest that abnormalities in the structure and function of the choroid are the main pathogenesis of CSC. However, the exact pathophysiological mechanism of CSC remains poorly understood.

The choroid primarily consists of the vascular layer, containing connective tissues, and lying between the retina and sclera. The structure of the vascular layer is divided into three layers: choriocapillaris consisting of capillaries; Sattler's layer consisting of small vessels; and Haller's layer consisting of medium and large vessels.[23] The rapid development of optical coherence tomography (OCT), such as enhanced depth imaging OCT[24] and swept-source (SS) OCT,[25] has made it possible to evaluate choroidal thickness and choroidal structure.[23] Using these techniques, several studies have proved that subfoveal choroidal thickness (SCT) is significantly greater in eyes with CSC than in normal eyes.[2,26] Chung et al.[27] subsequently reported that Haller's layer is significantly thicker in CSC eyes than in normal control eyes, whereas Sattler's layer is not significantly different. Furthermore, Sonoda et al.[28] used ImageJ software to analyze the choroidal structure by binarizing the choroid layers, classifying the luminal areas as black and the stromal areas as white. Using the binarization method, their research shows that the proportion of the luminal area (i.e., luminal/stromal [L/S] ratio) of the outer choroidal layer is significantly higher in CSC eyes compared with normal control eyes and fellow eyes.[28,29] These studies suggest that an

increase in the luminal area of the outer choroidal layer may have caused choroidal thickening in CSC eyes.

To date, it remains unclear how morphological factors affect choroidal structure in CSC eyes. Recently, using an anterior-segment (AS) OCT, we proposed that sclera may induce choroidal circulatory disturbances, based on the fact that CSC eyes had significantly thicker sclera than normal control eyes.[30,31] Unexpectedly, choroidal thickness did not simply correlate with scleral thickness in CSC eyes in our pilot study. To elucidate the relationship between scleral thickness and choroidal structure, we aimed to investigate the clinical factors related to the L/S ratio in the posterior choroid in CSC eyes.

Methods

This study was a retrospective case series performed at the University of the Ryukyus Hospital. The study was approved by the ethics committee of the University of the Ryukyus Hospital (approval number: 1503), and the investigation was carried according to the principles expressed in the Declaration of Helsinki. Informed consent was obtained from all patients participating in this study.

We retrospectively reviewed the medical records of 111 eyes of 111 consecutive patients (18 women and 93 men; mean age, 51.2 years; standard deviation [SD], 12.0 years) with CSC who initially visited the Macula Service of the University of the Ryukyus Hospital from October 2018 to August 2020. In cases of bilateral CSC, the right eye was selected.

CSC was diagnosed by the presence of SRD or pigment epithelial detachment involving the macula using SS OCT, the presence of SRD associated with leakage points at the level of retinal pigment epithelium (RPE) at the posterior pole on fluorescein angiography, and ICGA confirmed multifocal choroidal vascular hyperpermeability in the late phase. Exclusion criteria were the presence of other retinal diseases, including choroidal neovascularization, uveitis, ocular hypertension, and glaucoma; systemic corticosteroid therapy; systemic conditions associated with CSC; pregnancy; a history of intraocular surgery; a history of treatment for CSC including photocoagulation and photodynamic therapy; and poor image quality and inability to accurately analyze choroidal structure or scleral thickness.

At the initial visit, all 111 patients with CSC underwent comprehensive eye examinations, which included decimal best-corrected visual acuity testing with Landolt C charts, slit-lamp biomicroscopy of the anterior segment of the eye, and funduscopy using an ophthalmoscope. The objective refraction was measured by an autorefractor (ARK-1a; NIDEK, Gamagori, Japan), and spherical equivalent (SE) was calculated by the principal spherical power plus half of the cylindrical power. AL was measured with an interferometer (IOL Master 700; Carl Zeiss Meditec, La Jolla, CA, USA). Color fundus photography was performed by a fundus camera system (TRC-50DX; Topcon, Tokyo, Japan). Fluorescein angiography, ICGA, and fundus autofluorescence photography were obtained by using a confocal scanning laser ophthalmoscope (Spectralis HRA+OCT; Heidelberg Engineering, Heidelberg, Germany). We acquired cross-sectional images of the macular area using SS OCT (DRI-OCT Triton; Topcon, Tokyo, Japan). Using the caliper function of the EnView software (Enview, San Francisco, CA, USA) installed on the SS OCT, SCT was manually measured as the vertical distance from the hyper-reflective line corresponding to Bruch's membrane to the inner scleral border under the fovea. All patients underwent OCT angiography (Zeiss Plex Elite 9000; Carl Zeiss Meditec) to confirm the absence of macular neovascularization. Scleral thickness was measured with AS OCT (Casia 2; Tomey, Nagoya, Japan) in the same method as our previous reports (Fig. 1).[30–34] Briefly, the patient gazed in four directions (superior, temporal, inferior, and nasal), and AS OCT scans were taken along each rectus muscle with a diameter of 16 mm using a raster scan mode consisting of 16 B-scans with a width of 4 mm. Scleral thickness was measured using a B-scan image through the middle of each rectus muscle. The upper scleral line was determined by the low brightness of each rectus muscle, and the lower scleral line was delineated from the difference in brightness between sclera and choroid. Scleral thickness was vertically measured 6 mm posteriorly to the scleral spur in four directions.

Choroidal Binarization Methods

"EyeGround" software was used for choroidal structural analysis to calculate the L/S ratio of the choroid.[35] The B-scan image of the horizontal cross-section through the foveal center was obtained using SS OCT and converted to a TIFF image. The RPE layer was segmented automatically by the intensity adjustments of the software program. The border between the choroid and the sclera was manually

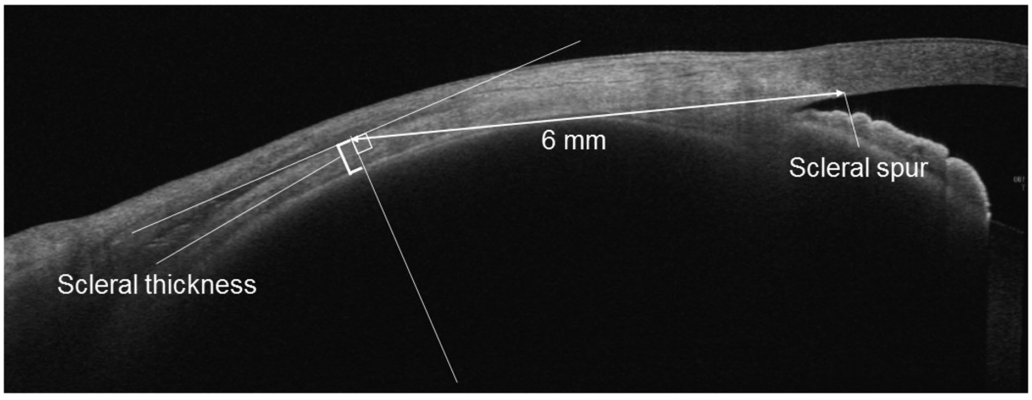

Figure 1. Scleral thickness measured using AS OCT images obtained by gazing at the opposite direction of the rectus muscles to be captured. The sclera was identified based on the brightness difference between the rectus muscle, the sclera and the choroid. Scleral thickness was measured vertically, 6 mm posterior to the scleral spur.

Investigative Ophthalmology & Visual Science

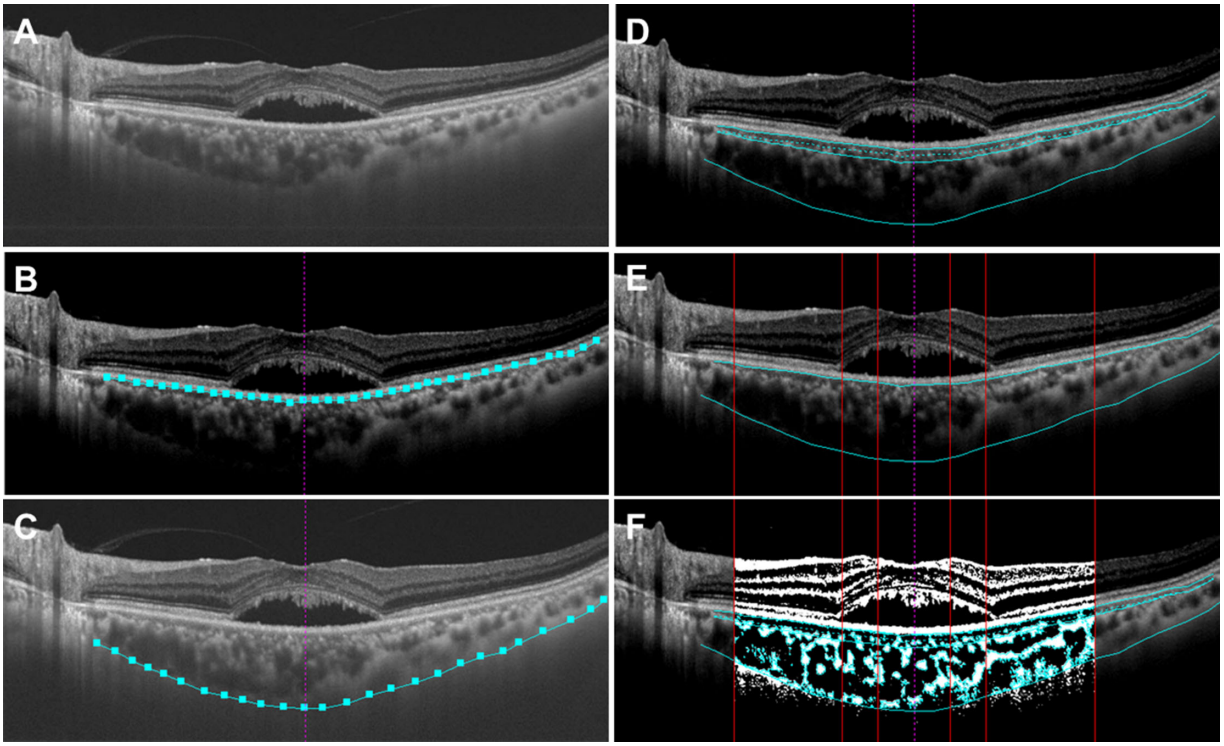

Figure 2. SS OCT images of the choroid converted to binarization images by semiautomated software "EyeGround." (**A**) The horizontal cross-sectional OCT image through the foveal center is converted to a TIFF image. (**B**) The RPE layer is segmented using the automatic discrimination of the software (*light blue square* and *line*). The *vertical purple dashed line* indicates the foveal center. (**C**) The chorioscleral border is manually segmented (*light blue square* and *line*). (**D**) The choroid is automatically divided into choriocapillaris, Sattler's layer, and Haller's layer. The *light blue dashed line* indicates the border between the choriocapillaris and the vascular layer. (**E**) The area of the choroid is demarcated into 1500 µm, 3000 µm, and 7500 µm ranges centered at the fovea (*vertical red lines*). (**F**) The images are binarized by the Niblack method and the L/S ratio is calculated from the luminal and stromal areas.

determined by the observer. The choroid was divided into choriocapillaris, Sattler's layer, and Haller's layer automatically. The software was programmed so that lines were drawn vertically to the RPE layer from the point closest to the RPE in five randomly selected large (>100 µm) luminal areas, and the mean length of these five lines was the border between Sattler's and Haller's layers. In this study, the SS OCT images of each case were evaluated for intrachoroidal structure (i.e., whole choroid [WC], inner choroid [IC], and outer choroid [OC]). The IC was defined as the choriocapillaris with Sattler's layer, and the OC was defined as Haller's layer. The SS OCT image of the choroidal area was binarized by the Niblack method automatically, and the black area was defined as the luminal area and the white area as the stromal area. The lowest cutoff value for binarization was defined as the average of the reflectance for the center of the three selected Haller's layer lumens regarded as the darkest by the original SS OCT image. This cutoff value was used as the reference of the lowest cutoff value for the brightness and binarization was performed. The L/S ratio of each case was evaluated for WC, IC, and OC at the ranges of 1500 µm, 3000 µm, and 7500 µm centered at the fovea on the horizontal cross-sectional image (Fig. 2).

Outcomes

The L/S ratios of all cases were calculated for WC, IC, and OC at the ranges of 1500 µm, 3000 µm, and 7500 µm centered at the fovea. The correlation between age, SE, AL, SCT, and the mean scleral thickness in four directions and the L/S ratios of WC, IC, and OC in each range were examined. Subsequently, if statistically significant correlation was shown, stepwise multiple regression analysis was used to analyze the relationship between gender, age, AL, SCT, and mean scleral thickness and L/S ratios.

Statistical Analysis

Spearman's rank correlation coefficient was used to calculate the correlation coefficient and P value. The results were expressed as mean ± SD. The association between gender, age, AL, SCT, and scleral thickness and the L/S ratio was assessed using multiple regression analysis, and partial regression coefficients and standard partial regression coefficients were calculated for significantly relevant factors. P values < 0.05 were considered to be statistically significant. All statistical data were analyzed using Statistical Analysis System software version 9.4 (SAS; SAS Inc., Cary, NC, USA).

Results

The clinical information of 111 eyes of 111 patients is summarized in Table 1. In all 111 eyes, SCT was 400.3 ± 100.6 µm, and scleral thickness was 421.9 ± 59.1 µm, 437.3

Table 1. Clinical Information of the Patients in the Choroidal Binarization Method

	Mean ± SD	Range
Number of eyes	111	
Age (yrs)	51.2 ± 12.0	28–83
Female, no (%)	18 (16.2%)	
Spherical equivalent (diopter)	−0.66 ± 1.97	−10.3 to 5.13
Axial length (mm)	23.57 ± 0.95	21.33–26.48
Subfoveal choroidal thickness (µm)	400.3 ± 100.6	152–637
Scleral thickness (µm)		
Mean	434.4 ± 47.2	321–559
Superior	421.9 ± 59.1	294–570
Temporal	437.3 ± 53.3	320–580
Inferior	445.5 ± 54.5	271–592
Nasal	433.2 ± 54.8	248–584

± 53.3 µm, 445.5 ± 54.5 µm, and 433.2 ± 54.8 µm in the superior, temporal, inferior, and nasal directions, respectively. The mean scleral thickness in the four directions was 434.4 ± 47.2 µm. In this cohort, the correlations between the mean scleral thickness and SCT was not significant ($R = 0.126$, $P = 0.185$).

The total choroidal area, luminal area, stromal area, and the L/S ratio at the 1500 µm, 3000 µm, and 7500 µm ranges centered at the fovea are shown in Table 2. The age and SE were not significantly correlated with the L/S ratio of WC, IC, and OC in all ranges. There was no significant correlation between AL and the L/S ratio in the 1500 µm and 3000 µm ranges. However, longer AL was significantly correlated with the reduction of the L/S ratio of WC ($R = -0.239$, $P = 0.014$) and OC ($R = -0.214$, $P = 0.028$) at the 7500 µm range (Table 3). Greater SCT was significantly correlated with the increased L/S ratio of WC and OC at the 1500 µm (WC: $R = 0.488$, $P < 0.001$; OC: $R = 0.437$, $P < 0.001$), 3000 µm (WC: $R = 0.423$, $P < 0.001$; OC: $R = 0.406$, $P < 0.001$), and 7500 µm (WC: $R = 0.414$, $P < 0.001$; OC: $R = 0.450$, $P < 0.001$) ranges, although there were no significant correlations between SCT and the L/S ratio of IC at all the other ranges (Table 3, Fig. 3). Similarly, the mean scleral thickness was significantly and positively correlated with the L/S ratio of WC and OC at 1500 µm (WC: $R = 0.558$, $P < 0.001$; OC: $R = 0561$, $P < 0.001$), 3000 µm (WC: $R = 0.592$, $P < 0.001$; OC: $R = 0.605$, $P < 0.001$), and 7500 µm (WC: $R = 0.541$, $P < 0.001$; OC: $R = 0.584$, $P < 0.001$) ranges, although there were no significant correlations between mean scleral thickness and the L/S ratio of IC at all the other ranges (Table 3, Fig. 4).

Stepwise multiple regression analysis in all cases showed that only SCT and mean scleral thicknesses were significantly and positively correlated with L/S ratio of WC and OC in all ranges. Standardized partial regression coefficient showed that SCT was the factor more significantly correlated

Table 2. Mean Value in Choroidal Area and Luminal/Stromal Ratio

	Total Choroidal Area (µm²)	Luminal Area (µm²)	Stromal Area (µm²)	Luminal/Stromal Ratio
Whole choroid				
1500 µm	620,071.8 ± 195,414.7	436,880.4 ± 142,640.4	183,191.5 ± 61,294.9	2.432 ± 0.517
3000 µm	1,226,427.8 ± 379,555.5	865,300.5 ± 274,713.3	361,127.3 ± 122,605.2	2.463 ± 0.603
7500 µm	2,771,491.3 ± 870,883.2	1,938,196.6 ± 626,129.8	833,294.8 ± 272,986.2	2.364 ± 0.478
Inner choroid				
1500 µm	198,455.1 ± 72,787.5	132,135.5 ± 48,173.4	66,319.6 ± 28,766.8	2.105 ± 0.607
3000 µm	391,661.6 ± 139,483.9	261,422.1 ± 90,629.2	130,239.5 ± 55,000.0	2.110 ± 0.505
7500 µm	882,662.3 ± 295,150.1	590,309.5 ± 192,558.6	292,352.7 ± 113,983.5	2.105 ± 0.430
Outer choroid				
1500 µm	421,616.8 ± 144,602.0	304,744.9 ± 108,958.4	116,871.9 ± 46,559.3	2.749 ± 0.896
3000 µm	834,766.2 ± 282,749.9	603,878.4 ± 210,631.4	230,887.8 ± 94,672.4	2.806 ± 1.080
7500 µm	1,888,829.1 ± 660,641.1	1,347,887.0 ± 485,341.2	540,942.0 ± 211,596.6	2.619 ± 0.939

Table 3. Correlation Between Age, Spherical Equivalent, Axial Length, Subfoveal Choroidal Thickness, Mean Scleral Thickness, and Luminal/Stromal Ratio

	Age		Spherical Equivalent (Diopter)		Axial Length (mm)		Subfoveal Choroidal Thickness (µm)		Mean Scleral Thickness (µm)	
	Correlation Coefficient	*P* Value	Correlation Coefficient	*P* Value	Correlation Coefficient	*P* Value	Correlation Coefficient	*P* Value	Correlation Coefficient	*P* Value
Whole choroid										
1500 µm	−0.074	0.442	0.187	0.054	−0.174	0.074	0.488	<0.001	0.558	<0.001
3000 µm	−0.101	0.292	0.131	0.179	−0.187	0.056	0.423	<0.001	0.592	<0.001
7500 µm	−0.137	0.152	0.092	0.344	−0.239	0.014	0.414	<0.001	0.541	<0.001
Inner choroid										
1500 µm	−0.129	0.177	−0.053	0.591	0.101	0.305	0.136	0.155	−0.012	0.901
3000 µm	−0.084	0.382	0.001	0.990	0.045	0.647	0.115	0.230	−0.048	0.619
7500 µm	−0.040	0.678	0.014	0.889	0.188	0.054	0.101	0.293	−0.084	0.381
Outer choroid										
1500 µm	−0.053	0.579	0.181	0.063	−0.075	0.446	0.437	<0.001	0.561	<0.001
3000 µm	−0.089	0.355	0.158	0.103	−0.126	0.200	0.406	<0.001	0.605	<0.001
7500 µm	−0.154	0.106	0.135	0.165	−0.214	0.028	0.449	<0.001	0.584	<0.001

Investigative Ophthalmology & Visual Science

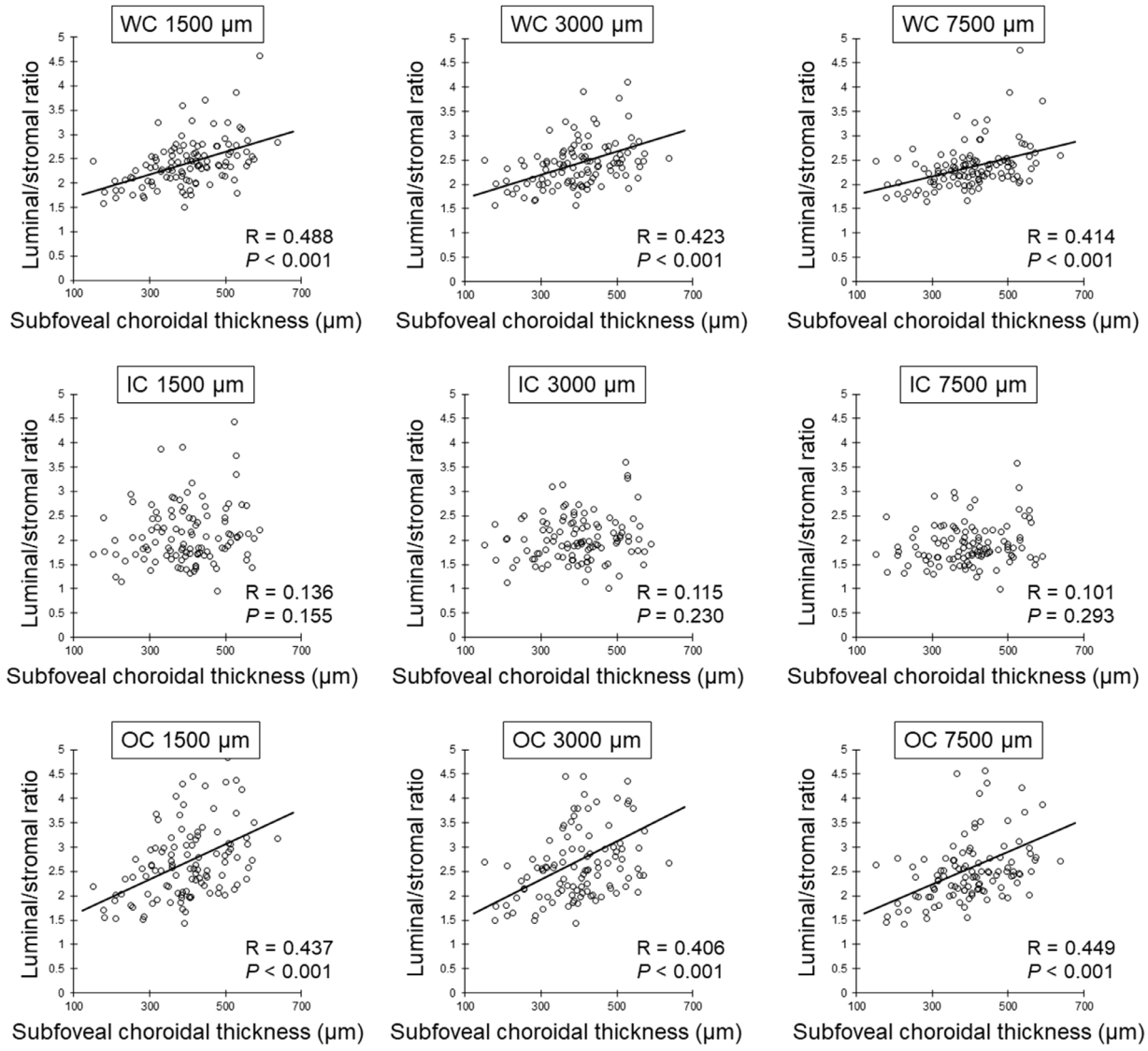

Figure 3. Relationship between SCT and L/S ratio by Spearman's rank correlation coefficient. SCT is significantly and positively correlated with the L/S ratio of WC and OC in all ranges.

with the increase in the L/S ratio of WC and OC at 1500 μm (WC: 0.522 vs. 0.437; OC: 0.523 vs. 0.466) and 3000 μm (WC: 0.441 vs. 0.426; OC: 0.453 vs. 0.447) ranges than mean scleral thickness. In contrast, mean scleral thickness was the factor significantly and more positively correlated with the increase in L/S ratio of WC and OC at 7500 μm range (WC: 0.386 vs. 0.368; OC: 0.391 vs. 0.383) than SCT (Table 4).

Discussion

This study demonstrated that SCT and mean scleral thickness were significantly and positively correlated with L/S ratio in all ranges of WC and OC. Multiple regression analysis found that SCT and mean scleral thickness were significantly correlated with the L/S ratio, and the strength of correlation of mean scleral thickness was greater than that of SCT in the 7500 μm range.

It has been reported that choroidal structural analysis converted to binarization by the Niblack method has shown high reproducibility.[28,35] In this study, by using automated choroidal structure analysis software, "EyeGround," with maximizing the automation mode, we examined the clinical factors associated with choroidal structure in CSC patients. As a result, we have revealed that thick choroid and thick sclera were significantly correlated to an increase in the L/S ratio of WC and OC in the posterior pole. In contrast, the L/S ratio of IC had no correlation with clinical factors such as SCT or scleral thickness. To our knowledge, no previous studies have reported these results regarding the choroidal structural analysis of CSC.

In this study, SCT and the L/S ratio were significantly and positively correlated in the posterior pole of CSC eyes. Additionally, about half of the CSC eyes had an L/S ratio of 2.4 or higher in WC and OC, which tended to be higher than that of normal control eyes in previous reports.[29,36] These results suggested that the cause of choroidal thickening in CSC eyes might be an increase in the luminal component of the outer choroidal layer. Agrawal et al.[37] binarized the choroid into luminal and stromal areas by spectral-domain OCT and reported that the luminal areas were significantly

Investigative Ophthalmology & Visual Science

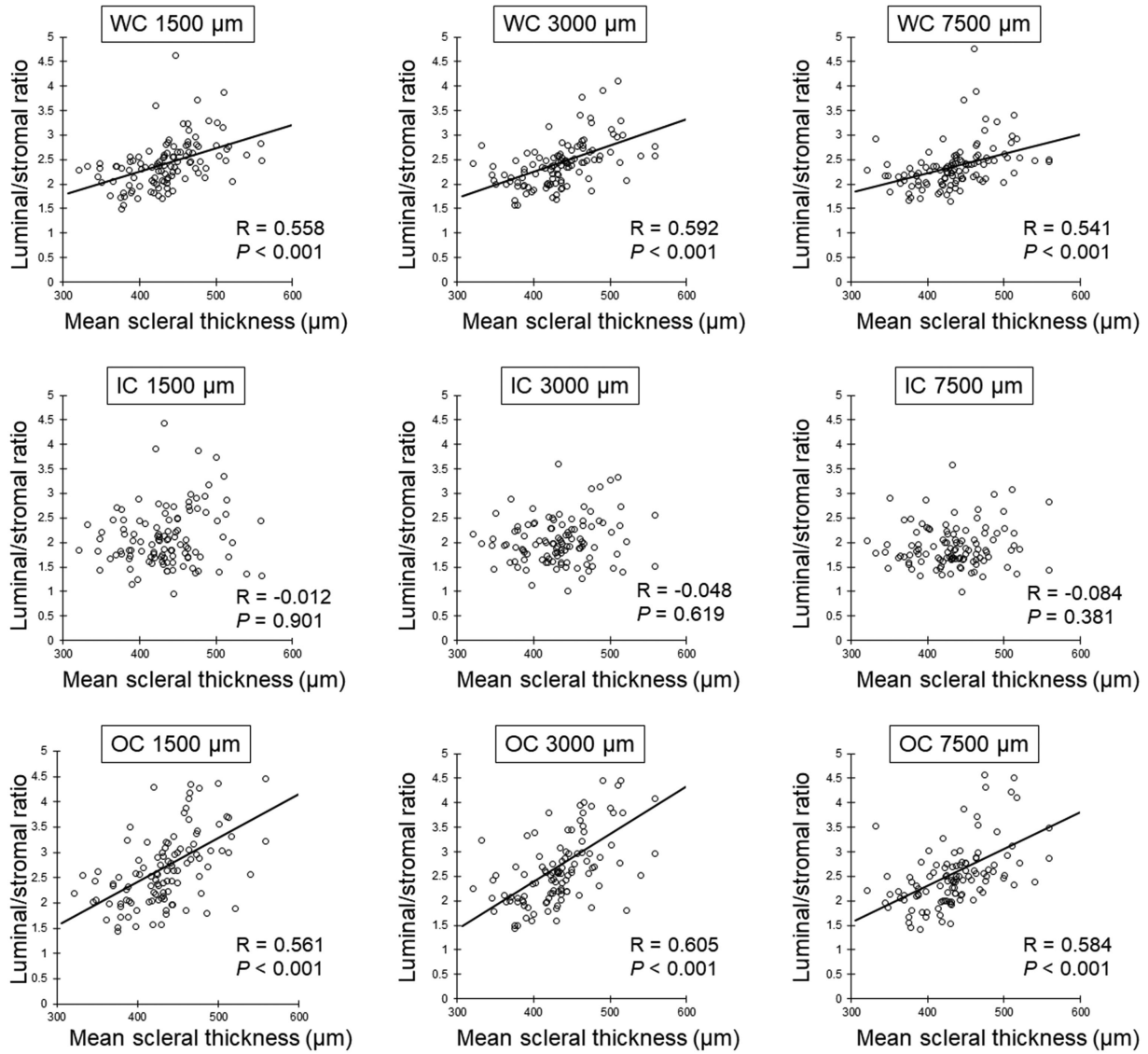

Figure 4. Relationship between mean scleral thickness and L/S ratio by Spearman's rank correlation coefficient. Mean scleral thickness is significantly and positively correlated with the L/S ratio of WC and OC in all ranges.

larger than the stromal areas in CSC eyes. In addition, the increased luminal areas were noted in CSC eyes in comparison with age-matched healthy subjects.[37] Similarly, Sonoda et al.[29] reported that the luminal area of the outer choroidal layer was significantly larger than the stromal area and had a higher L/S ratio in CSC eyes than in normal eyes. These results are consistent with ours. Furthermore, Sonoda et al.[36] reported that the L/S ratio decreased significantly with increasing age and longer AL in normal eyes. In this study, age and SE did not significantly correlate with the L/S ratio in CSC eyes, whereas AL was significantly correlated only at the 7500 µm range, but the correlation coefficient was lower than their report. These results show that the effects of age, SE, and AL on the L/S ratio are less in CSC eyes than in normal eyes, and other factors may define the L/S ratio.

Recently, using AS OCT, we demonstrated that CSC eyes had significantly thicker sclera than normal control eyes, suggesting an overlap with the pathogenesis of uveal effusion syndrome,[30] and subsequent reports supported our finding.[31,38,39] CSC and uveal effusion syndrome characterized by thick sclera share the same clinical features, such as a thick choroid and SRD.[40,41] Choroidal blood flow is excreted out of the eye by four or more vortex veins. The thick sclera increases the vascular resistance of the penetrating vortex veins and may cause stasis of the choroidal blood flow. Vortex vein congestion was shown in wide-field ICGA[21] and en face OCT[42] as dilatation of the outer choroidal layer vessels. Further, a study with laser speckle flowgraphy demonstrated that reduced blood flow velocity in the asymmetrically dilated vortex veins in pachychoroid spectrum diseases, suggesting the anatomical vascular congestions.[43] Additionally, the thick sclera may reduce the trans-scleral outflow of choroidal fluid and prevent excessive fluid from being excreted through the sclera. These choroidal excretion pathways may be disturbed by thick sclera, resulting in vasodilation of the outer choroidal layer. In the present study, scleral thickness was positively correlated with the L/S ratio in WC and OC, suggesting that scleral thickening contributes to the increase in the choroidal luminal components. The thicker sclera may increase the luminal area of the

Table 4. Results of Stepwise Multiple Regression Analysis to The Ratio of Luminal to Stromal Area in The Choroidal Binarization Method

Variables	Partial Regression Coefficient	Standardized Partial Regression Coefficient	*P* Value
Whole choroid			
1500 µm			
Subfoveal choroidal thickness (µm)	0.003	0.522	<0.0001
Mean scleral thickness (µm)	0.005	0.437	<0.0001
Constant	−2.114		
Adjusted R^2	0.402		
3000 µm			
Subfoveal choroidal thickness (µm)	0.003	0.441	<0.0001
Mean scleral thickness (µm)	0.006	0.426	<0.0001
Constant	−2.439		
Adjusted R^2	0.329		
7500 µm			
Subfoveal choroidal thickness (µm)	0.002	0.368	0.0004
Mean scleral thickness (µm)	0.004	0.386	<0.0001
Constant	0.510		
Adjusted R^2	0.290		
Outer choroid			
1500 µm			
Subfoveal choroidal thickness (µm)	0.004	0.523	<0.0001
Mean scleral thickness (µm)	0.008	0.466	<0.0001
Constant	−5.964		
Adjusted R^2	0.418		
3000 µm			
Subfoveal choroidal thickness (µm)	0.004	0.453	<0.0001
Mean scleral thickness (µm)	0.009	0.447	<0.0001
Constant	−5.656		
Adjusted R^2	0.359		
7500 µm			
Subfoveal choroidal thickness (µm)	0.003	0.383	0.0002
Mean scleral thickness (µm)	0.007	0.391	<0.0001
Constant	−1.267		
Adjusted R^2	0.335		

choroid in OC and consequently increase the entire thickness of the choroid. However, this study demonstrated that the thicker sclera did not simply result in a thicker choroid. Besides, the maximum limit of choroidal thickness seems to have individual differences, because the variation of SCT increases as the L/S ratio increases in the scatter plot of SCT and the L/S ratio. Therefore the choroidal venous overload by thick sclera needs to be further investigated.[44]

In the current study, we demonstrated that scleral thickening, as well as greater SCT, contributed to the increased L/S ratio by stepwise multiple regression analysis. However, the correlation coefficient between the mean scleral thickness and the L/S ratio of WC and OC was less than 0.6. In this respect, the choroidal abnormality in CSC eyes may be affected by variable factors, not just scleral thickness. Using laser speckle flowgraphy, Saito et al.[45] reported the increase in choroidal blood flow in the acute CSC and the increase in vascular resistance at the site of delayed filling on ICGA. They presumed that the changes in choroidal blood flow was due to sympathetic hyperactivity.[46] CSC has risk factors such as type-A behavior,[6] psychic stress,[7] hypertension,[5] and smoking,[5] and the involvement of sympathetic hyperactivity is generally supported. These findings indicate that pachychoroid status in CSC eyes is due to the combination of physiological dynamic and anatomical static factors. It requires further studies to clarify the extent to which the thick sclera of CSC eyes affects choroidal structure and circulation.

The advantage of this study is that the structural analysis of the choroid was done semi-automatically, and manual bias was almost eliminated. Additionally, the software used in the analysis has already been proven to have excellent reproducibility and repeatability.[35] However, there are also several limitations. First, the CSC cases in this study mainly consisted of severe cases referred for treatments, thereby mild CSC cases were excluded. Clinical factors related to choroidal structure in normal control eyes and pachychoroid spectrum disease eyes other than CSC need to be investigated further. Second, the measurements of choroidal and scleral thicknesses were performed manually since there was no automated software available. Third, it was impossible to clearly separate the choroidal luminal areas from the loculation of fluid[34,47] in our binarization method. Although the loculation of fluid is much smaller than the choroidal luminal areas, the L/S ratio in this study did not completely reflect the choroidal luminal and stromal areas. Finally, with present AS OCT, it was impossible to obtain the deeper scleral image such as the trans-scleral parts of the vortex vein. The morphological features of the vortex veins at the site penetrating the sclera remain unknown.

In conclusion, this study analyzed clinical factors related to the structural changes of the choroid in CSC eyes. The results showed that SCT and scleral thickness in CSC eyes were significantly and positively correlated with increased choroidal luminal components in the WC and OC. The effects of SCT and scleral thickness on choroidal luminal

components were independently associated, and effects of these on choroidal luminal components were comparable. Our findings may provide further strong evidence for the close relationship between the choroid and sclera in CSC pathology. Further studies using ultra-wide-field ICGA or more extensive choroidal B-scan and en face images are required to determine how the sclera affects the choroid.

Acknowledgments

The authors thank Editage (www.editage.com) for the English language editing.

Supported by JSPS KAKENHI Grant Number JP20K18349.

Disclosure: **N. Imanaga**, None; **N. Terao**, None; **S. Sonoda**, None; **S. Sawaguchi**, None; **Y. Yamauchi**, None; **T. Sakamoto**, None; **H. Koizumi**, None

References

1. van Rijssen TJ, van Dijk EHC, Yzer S, et al. Central serous chorioretinopathy: Towards an evidence-based treatment guideline. *Prog Retin Eye Res*. 2019;73:100770.
2. Cheung CMG, Lee WK, Koizumi H, Dansingani K, Lai TYY, Freund KB. Pachychoroid disease. *Eye (Lond)*. 2019;33:14–33.
3. Tittl MK, Spaide RF, Wong D, et al. Systemic findings associated with central serous chorioretinopathy. *Am J Ophthalmol*. 1999;128:63–68.
4. Kitzmann AS, Pulido JS, Diehl NN, Hodge DO, Burke JP. The incidence of central serous chorioretinopathy in Olmsted County, Minnesota, 1980-2002. *Ophthalmology*. 2008;115:169–173.
5. Ersoz MG, Arf S, Hocaoglu M, Sayman Muslubas I, Karacorlu M. Patient characteristics and risk factors for central serous chorioretinopathy: an analysis of 811 patients. *Br J Ophthalmol*. 2019;103:725–729.
6. Yannuzzi LA. Type-A behavior and central serous chorioretinopathy. *Retina*. 1987;7:111–131.
7. Spahn C, Wiek J, Burger T, Hansen L. Psychosomatic aspects in patients with central serous chorioretinopathy. *Br J Ophthalmol*. 2003;87:704–708.
8. Haimovici R, Koh S, Gagnon DR, Lehrfeld T, Wellik S, Central Serous Chorioretinopathy Case-Control Study G. Risk factors for central serous chorioretinopathy: a case-control study. *Ophthalmology*. 2004;111:244–249.
9. Sunness JS. The pregnant woman's eye. *Surv Ophthalmol*. 1988;32:219–238.
10. Oh JH, Oh J, Togloom A, Kim SW, Huh K. Biometric characteristics of eyes with central serous chorioretinopathy. *Invest Ophthalmol Vis Sci*. 2014;55:1502–1508.
11. Terao N, Koizumi H, Kojima K, et al. Short axial length and hyperopic refractive error are risk factors of central serous chorioretinopathy. *Br J Ophthalmol*. 2020;104:1260–1265.
12. Miki A, Kondo N, Yanagisawa S, Bessho H, Honda S, Negi A. Common variants in the complement factor H gene confer genetic susceptibility to central serous chorioretinopathy. *Ophthalmology*. 2014;121:1067–1072.
13. Hosoda Y, Yoshikawa M, Miyake M, et al. CFH and VIPR2 as susceptibility loci in choroidal thickness and pachychoroid disease central serous chorioretinopathy. *Proc Natl Acad Sci U S A*. 2018;115:6261–6266.
14. van Dijk EHC, Schellevis RL, van Bergen M, et al. Association of a haplotype in the NR3C2 gene, encoding the mineralocorticoid receptor, with chronic central serous chorioretinopathy. *JAMA Ophthalmol*. 2017;135:446–451.
15. de Jong EK, Breukink MB, Schellevis RL, et al. Chronic central serous chorioretinopathy is associated with genetic variants implicated in age-related macular degeneration. *Ophthalmology*. 2015;122:562–570.
16. Hosoda Y, Miyake M, Schellevis RL, et al. Genome-wide association analyses identify two susceptibility loci for pachychoroid disease central serous chorioretinopathy. *Commun Biol*. 2019;2:468.
17. Gass JD. Pathogenesis of disciform detachment of the neuroepithelium. *Am J Ophthalmol*. 1967;63:617/645–644/672.
18. Hayashi K, Hasegawa Y, Tokoro T. Indocyanine green angiography of central serous chorioretinopathy. *Int Ophthalmol*. 1986;9:37–41.
19. Piccolino FC, Borgia L. Central serous chorioretinopathy and indocyanine green angiography. *Retina*. 1994;14:231–242.
20. Spaide RF, Hall L, Haas A, et al. Indocyanine green videoangiography of older patients with central serous chorioretinopathy. *Retina*. 1996;16:203–213.
21. Pang CE, Shah VP, Sarraf D, Freund KB. Ultra-widefield imaging with autofluorescence and indocyanine green angiography in central serous chorioretinopathy. *Am J Ophthalmol*. 2014;158:362–371.e362.
22. Hirahara S, Yasukawa T, Kominami A, Nozaki M, Ogura Y. Densitometry of Choroidal Vessels in Eyes With and Without Central Serous Chorioretinopathy by Wide-Field Indocyanine Green Angiography. *Am J Ophthalmol*. 2016;166:103–111.
23. Staurenghi G, Sadda S, Chakravarthy U, Spaide RF, International Nomenclature for Optical Coherence Tomography P. Proposed lexicon for anatomic landmarks in normal posterior segment spectral-domain optical coherence tomography: the IN*OCT consensus. *Ophthalmology*. 2014;121:1572–1578.
24. Spaide RF, Koizumi H, Pozzoni MC. Enhanced depth imaging spectral-domain optical coherence tomography. *Am J Ophthalmol*. 2008;146:496–500.
25. Yasuno Y, Hong Y, Makita S, et al. In vivo high-contrast imaging of deep posterior eye by 1-microm swept source optical coherence tomography and scattering optical coherence angiography. *Opt Express*. 2007;15:6121–6139.
26. Imamura Y, Fujiwara T, Margolis R, Spaide RF. Enhanced depth imaging optical coherence tomography of the choroid in central serous chorioretinopathy. *Retina*. 2009;29:1469–1473.
27. Chung YR, Kim JW, Kim SW, Lee K. Choroidal thickness in patients with central serous chorioretinopathy: assessment of Haller and Sattler layers. *Retina*. 2016;36:1652–1657.
28. Sonoda S, Sakamoto T, Yamashita T, et al. Choroidal structure in normal eyes and after photodynamic therapy determined by binarization of optical coherence tomographic images. *Invest Ophthalmol Vis Sci*. 2014;55:3893–3899.
29. Sonoda S, Sakamoto T, Kuroiwa N, et al. Structural changes of inner and outer choroid in central serous chorioretinopathy determined by optical coherence tomography. *PloS One*. 2016;11:e0157190.
30. Imanaga N, Terao N, Nakamine S, et al. Scleral thickness in central serous chorioretinopathy. *Ophthalmol Retina*. 2021;5:285–291.
31. Terao N, Imanaga N, Wakugawa S, et al. Ciliochoroidal effusion in central serous chorioretinopathy. *Retina*. 2022;42:730–737.
32. Terao N, Imanaga N, Wakugawa S, et al. Short axial length is related to asymmetric vortex veins in central serous chorioretinopathy. *Ophthalmol Sci*. 2021;1:100071.
33. Sawaguchi S, Terao N, Imanaga N, et al. Scleral thickness in steroid-induced central serous chorioretinopathy. *Ophthalmol Sci*. 2022;2:100124.

34. Imanaga N, Terao N, Sawaguchi S, et al. Clinical factors related to loculation of fluid in central serous chorioretinopathy. *Am J Ophthalmol*. 2022;235:197–203.
35. Sonoda S, Sakamoto T, Kakiuchi N, et al. Semi-automated software to measure luminal and stromal areas of choroid in optical coherence tomographic images. *Jpn J Ophthalmol*. 2018;62:179–185.
36. Sonoda S, Sakamoto T, Yamashita T, et al. Luminal and stromal areas of choroid determined by binarization method of optical coherence tomographic images. *Am J Ophthalmol*. 2015;159:1123–1131.e1121.
37. Agrawal R, Chhablani J, Tan KA, Shah S, Sarvaiya C, Banker A. Choroidal vascularity index in central serous chorioretinopathy. *Retina*. 2016;36:1646–1651.
38. Lee YJ, Lee YJ, Lee JY, Lee S. A pilot study of scleral thickness in central serous chorioretinopathy using anterior segment optical coherence tomography. *Sci Rep*. 2021;11:5872.
39. Fernandez-Vigo JI, Moreno-Morillo FJ, Shi H, et al. Assessment of the anterior scleral thickness in central serous chorioretinopathy patients by optical coherence tomography. *Jpn J Ophthalmol*. 2021;65:769–776.
40. Elagouz M, Stanescu-Segall D, Jackson TL. Uveal effusion syndrome. *Survey of ophthalmology*. 2010;55:134–145.
41. Boulanger E, Bonnin S, Delahaye-Mazza C, Tadayoni R, Gaudric A. Central serous chorioretinopathy mimicking idiopathic uveal effusion syndrome [published online ahead of print June 1, 2021]. *Retin Cases Brief Rep*, doi:10.1097/ICB.0000000000001170.
42. Hiroe T, Kishi S. Dilatation of asymmetric vortex vein in central serous chorioretinopathy. *Ophthalmol Retina*. 2018;2:152–161.
43. Hirooka K, Saito M, Yamashita Y, et al. Imbalanced choroidal circulation in eyes with asymmetric dilated vortex vein. *Jpn J Ophthalmol*. 2022;66:14–18.
44. Spaide RF, Gemmy Cheung CM, Matsumoto H, et al. Venous overload choroidopathy: a hypothetical framework for central serous chorioretinopathy and allied disorders. *Prog Retin Eye Res*. 2022;86:100973.
45. Saito M, Saito W, Hashimoto Y, et al. Macular choroidal blood flow velocity decreases with regression of acute central serous chorioretinopathy. *Br J Ophthalmol*. 2013;97:775–780.
46. Saito M, Saito W, Hirooka K, et al. Pulse waveform changes in macular choroidal hemodynamics with regression of acute central serous chorioretinopathy. *Invest Ophthalmol Vis Sci*. 2015;56:6515–6522.
47. Spaide RF, Ryan EH. Loculation of fluid in the posterior choroid in eyes with central serous chorioretinopathy. *Am J Ophthalmol*. 2015;160:1211–1216.